

Thermal spin-transfer in Fe-MgO-Fe tunnel junctions

Xingtao Jia and Ke Xia

Department of Physics, Beijing Normal University, Beijing 100875, China

Gerrit E. W. Bauer

Institute for Materials Research, Tohoku University, Sendai 980-8577, Japan and
Delft University of Technology, Kavli Institute of NanoScience, 2628 CJ Delft, The Netherlands

(Dated: May 5, 2022)

We compute thermal spin transfer torques (TST) in Fe-MgO-Fe tunnel junctions using a first principles wave function-matching method. At room temperature, the TST in a junction with 3 MgO monolayers amounts to 10^{-7} J/m²/K, which is estimated to cause magnetization reversal for temperature differences over the barrier of the order of 10 K. The large TST can be explained by multiple scattering between interface states through ultrathin barriers. The angular dependence of the TST can be very skewed, possibly leading to thermally induced high-frequency generation.

PACS numbers: 72.25.Ba, 85.75.-d, 72.10.Bg

Spin-dependent thermoelectric effects in metallic magnetic systems have been known for quite some time [1] but recently experience renewed interest. Spin caloritronic phenomena [2] include the spin Seebeck effect [3], which should be distinguished from the spin-dependent Seebeck effect in nanostructures [4]. Large spin-related Peltier cooling effects have been measured in magnetic NiCu nanopillars [5]. Hatami *et al.* [6] predicted that a temperature gradient induces a spin transfer torque that can excite a magnetization. Experimental evidence for the thermal spin-transfer torque has been obtained for Co-Cu-Co nanowires [7]. Slonczewski recently argued that thermal torques can be generated efficiently in spin valves with polarizing magnetic insulators [8].

Magnetic tunnel junctions (MTJs) of transition metals with MgO barriers [9, 10] have great potential for applications in magnetic random access memory (MRAM) elements and high-frequency generators [11–14]. An important goal of academic and corporate research remains the reduction of the critical currents necessary to induce magnetization precession and reversal [15, 16]. Spin-dependent Seebeck effects in MTJs have very recently been computed [17] and measured [18]. A spin accumulation has been injected thermally into silicon by permalloy contacts through MgO tunnel junctions [19].

Here we predict very large thermal spin transfer torques in MTJs with thin MgO barriers, which might open new possibilities to design memory elements and high-frequency generators driven by heat currents only. We have been motivated by the strong energy dependence of electron transmission through MTJs with thin barriers due to the existence of interface resonant states [20], which should cause large thermoelectric effects. Focussing on epitaxial Fe-MgO-Fe MTJs under a temperature bias, we demonstrate the effectiveness of thermal spin transfer torques by *ab initio* calculations based on the Landauer-Büttiker transport formalism. Consider an

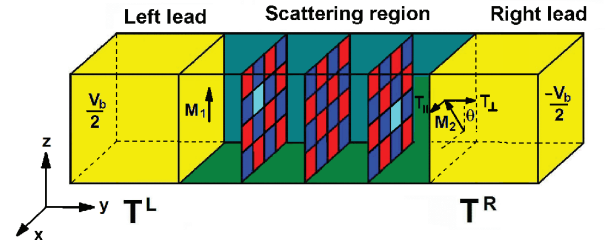


FIG. 1: Schematic Fe-MgO(3ML)-Fe(001) MTJs. We consider both a temperature difference ΔT and voltage difference V_b between the ferromagnetic reservoirs. The magnetization \mathbf{M}_1 of the left lead is fixed along the z -axis, while the magnetization \mathbf{M}_2 of the right lead is rotated by an angle θ in the xz plane relative to \mathbf{M}_1 . The small dark gray (red and dark blue) squares in the scattering region represent O and Mg atoms, respectively, while the light gray (light blue) ones denote oxygen vacancies.

MTJ as sketched in Fig. 1 with a voltage and temperature bias over the two leads, which are in local thermal equilibrium with Fermi-Dirac distribution functions $f_{L/R}(\epsilon) = [e^{(\epsilon - \mu_{L/R})/k_B T_{L/R}} + 1]^{-1}$ and local chemical potentials $\mu_{L/R}$ and temperatures $T_{L/R}$. The generalized Landauer-Büttiker formalism [21] is very suitable to handle transport through layered magnetic structures. The spin current from the n -th layer to the $n+1$ -th layer can be written as [22]

$$\mathbf{J}_{n+1,n} = \frac{1}{8\pi} \int d\epsilon [\mathbf{t}_{n+1,n}^L(\epsilon) f_L(\epsilon) + \mathbf{t}_{n,n+1}^R(\epsilon) f_R(\epsilon)] . \quad (1)$$

Here the energy-dependent spin transmission coefficient matrix from the left (right) direction is defined as $\mathbf{t}_{n+1,n}^{L/R}(\epsilon) = \sum_{\mathbf{k}_{\parallel}} \langle \Psi_{\mathbf{k}_{\parallel}}^{L/R}(\epsilon) | \hat{\mathcal{J}}_{n+1,n}(\mathbf{k}_{\parallel}) | \Psi_{\mathbf{k}_{\parallel}}^{L/R}(\epsilon) \rangle$ with spin current operator $\hbar \hat{\mathcal{J}}_{n+1,n}(\mathbf{k}_{\parallel}) = -\text{Re} \sum_{L,L'} \{ \hat{\sigma}, \hat{H}_{nL,n+1L'}(\mathbf{k}_{\parallel}) \}$, $\hat{H}_{nL,n+1L'}(\mathbf{k}_{\parallel})$ denotes the Hamiltonian matrix in spin space [22], where

$L \equiv (l, m)$ are the azimuthal and magnetic quantum numbers. $\hat{\sigma}$ is the vector of Pauli spin matrices and \mathbf{k}_{\parallel} is integrated over the two-dimensional Brillouin zone of transverse modes.

When the applied voltage vanishes and $k_B \Delta T \ll \epsilon_F$ we may expand Eq. (1) in $\Delta T = T_R - T_L$.

$$\mathbf{J}_{n+1,n} = \frac{1}{8\pi} \left\{ \int d\epsilon f(\epsilon_F, T_0) [\mathbf{t}_{n+1,n}^L(\epsilon) + \mathbf{t}_{n,n+1}^R(\epsilon)] + \frac{\Delta T}{2T_0} \int d\epsilon (\epsilon - \epsilon_F) \frac{\partial f}{\partial \epsilon} [\mathbf{t}_{n+1,n}^L(\epsilon) - \mathbf{t}_{n,n+1}^R(\epsilon)] \right\}, \quad (2)$$

where $T_0 \equiv (T^L + T^R)/2$. The first term in $\mathbf{J}_{n+1,n} = \mathbf{J}_{n+1,n}^{eq} + \mathbf{J}_{n+1,n}^{\Delta T}$ is the equilibrium spin current that communicates the exchange coupling through the barrier, while $\mathbf{J}_{n+1,n}^{\Delta T}$ is the thermal spin current. The torque acting on the n -th layer is the difference between the incoming and outgoing spin currents $\mathbf{T}_n^{\Delta T} = \mathbf{J}_{n,n-1}^{\Delta T} - \mathbf{J}_{n+1,n}^{\Delta T}$. The total thermal spin transfer (TST) torque is then

$$\mathbf{T}_{\Delta T} = \frac{\Delta T}{eT_0} \int d\epsilon (\epsilon - \epsilon_F) \tau_V(\epsilon) \frac{\partial}{\partial \epsilon} f(\epsilon), \quad (3)$$

where $\tau_V(\epsilon) = (e/16\pi) \sum_{n=N}^{\infty} [\mathbf{t}_{n,n-1}^L(\epsilon) - \mathbf{t}_{n-1,n}^R(\epsilon) - \mathbf{t}_{n+1,n}^L(\epsilon) + \mathbf{t}_{n,n+1}^R(\epsilon)]$ is the electrical torkance, and the sum from N to ∞ runs from the first layer at the interface until deep into the bulk of the “free” magnetic lead. The thermal torkance $\tau_T = \mathbf{T}_{\Delta T}/\Delta T$ depends on the energy dependent transmission and T_0 . Only when $\tau_V(\epsilon)$ varies slowly around the Fermi level in the thermal window $k_B \Delta T$, the Sommerfeld expansion may be employed and $\tau_T \rightarrow -(e/2) (\pi^2 k_B^2 T_0 / 6) \partial \tau_V(\epsilon) |_{\epsilon_F}$. For comparison, the linear-response voltage-driven torkance reads [22] $\mathbf{T}_{\Delta V} \Delta V(\epsilon_F)/V_b \rightarrow \tau_V(\epsilon_F)$, where V_b is the applied bias. We found that Eq. (3) accurately reproduces non-linear calculations based on Eq. (1) in the parameter regime considered here.

Here we focus mainly on Fe-MgO-Fe(100) with 3 layers (3L) MgO (~ 6 Å), corresponding to the thinnest barrier that can be reliably grown [11–14]. Ignoring the small lattice mismatch between the lead and barriers, we assume an isomorphous structure with unrelaxed interfacial atoms at bcc positions. We use a 1200×1200 k -point mesh in the full two-dimensional Brillouin zone (BZ) of transport channels to ensure numerical convergence. Details of the electronic structure and transport calculations can be found elsewhere [23].

The energy-dependent transmission through our MTJ is plotted in Fig. 2 for the parallel (P) and antiparallel (AP) configurations. Vacancies break the crystalline symmetry [24], broaden the resonant peaks of the minority spin channel, and enhance the coupling between majority Δ_1 state of one lead and the surface states of the minority spin on the other side. The newly opened channels increase the AP conductance.

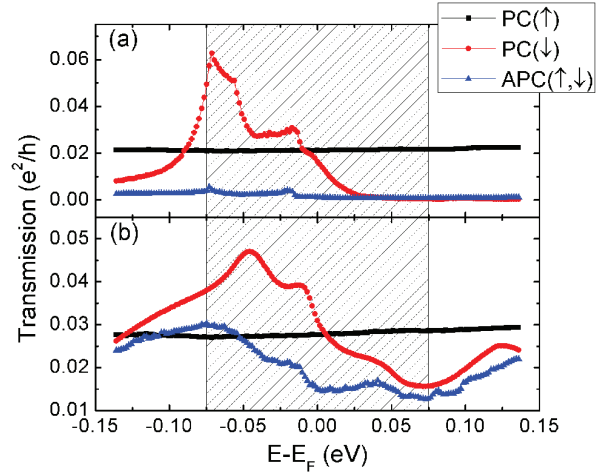


FIG. 2: Energy-dependent transmission of Fe-MgO(3L)-Fe(001) MTJs with (a) perfect interfaces and (b) 10% OVs at both interfaces. The shaded area indicates the thermal energy window $k_B T_0$ at room temperature.

For specular Fe-MgO interfaces, we find a zero-bias “optimistic” tunneling magnetoresistance (TMR) of 1300% and a resistance area $0.063 \Omega \mu\text{m}^2$. Our TMR ratio is consistent with a “pessimistic” TMR calculated to be around 0.93 for the same barrier thickness [25] with majority-spin transmission around $0.4e^2/h$ [26]. When 10% oxygen vacancies (OVs) (the energetically most favorable defects) are introduced at the interface, the TMR decreases to 96% and $RA = 0.036 \Omega \mu\text{m}^2$. When 10% OVs are introduced in the middle of barrier, the TMR drops to 70%, and the RA slightly increases to $0.076 \Omega \mu\text{m}^2$. These results are comparable with the measured $0.19 \Omega \mu\text{m}^2$ and TMR = 15% for a similar barrier thickness at room temperature [13].

From the energy-dependent transmissions, we can also compute the magneto Seebeck coefficients [17] and electronic heat conductances. At $T = 10$ K, we find $\chi_e^P = 2.1 \times 10^6 \text{ W K}^{-1} \text{ m}^{-2}$ and $\chi_e^{AP} = 0.14 \times 10^6 \text{ W K}^{-1} \text{ m}^{-2}$, which, including estimated phonon contributions to the heat conductance, leads to the thermoelectric figure of merit $(ZT)_{10\text{K}} \simeq 10^{-3}$.

In Fig. 3 (a) and (b), we present the in- and out-of-plane angular-resolved torkances of specular Fe-MgO(3L)-Fe MTJs. The in-plane torkance is smooth in most energy regions, indicating good numerical convergence. We observe two resonances: a small one at $E_F - 0.02$ eV that contributes to the TST for $T_0 \gtrsim 100$ K and a sharp and larger peak at $E_F - 0.0725$ eV that contributes to the TST for $T_0 \gtrsim 300$ K. The out-of-plane torkance is much more sensitive to numerical details. The noise in Fig. 3 does not affect the integrated TST, however. At energies far away from the Fermi level ($E \geq E_F + 0.03$ eV and $E \leq E_F - 0.09$ eV), the in-plane torkance is small and proportional to $\sin \theta$ as predicted

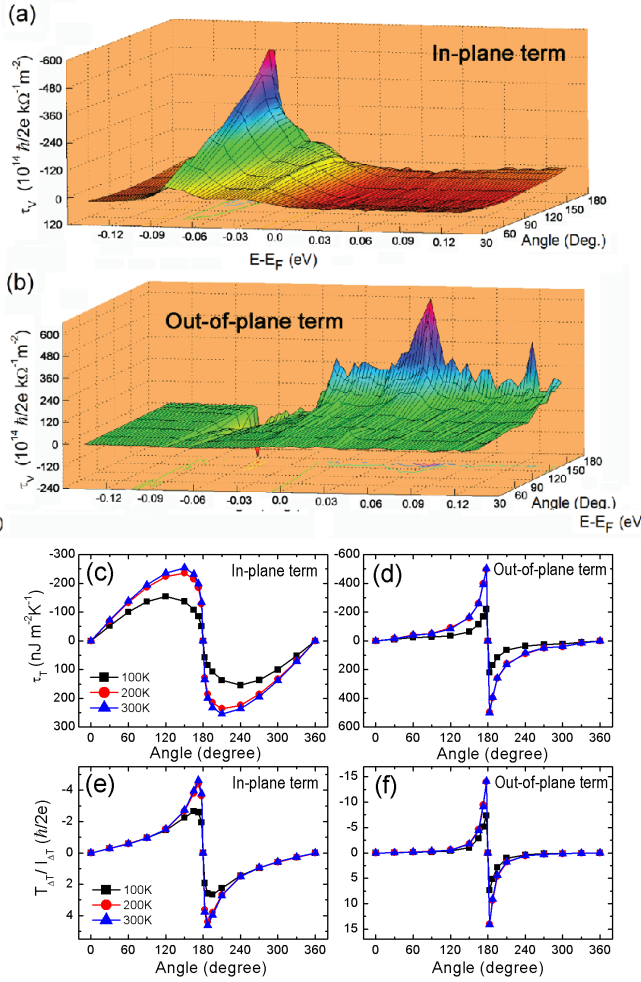


FIG. 3: Energy and angle-dependent (a) in-plane and (b) out-of-plane torkance, angular dependent (c) in-plane and (d) out-of-plane TST, and ratio of (e) in-plane and (f) out-of-plane TST to thermocurrent ($T_{\Delta T}/I_{\Delta T}$) of epitaxial Fe-MgO(3L)-Fe(001) MTJs.

by model studies [27]. However, this region contributes only weakly to the TST. The two sharp peaks near the Fermi level show an angular dependence that deviates strongly from a sine function. The asymmetry of the angular dependence of the in-plane TST reflects multiple scattering in the barrier and is therefore exponentially suppressed for thick layers. The in-plane TST of 7L MTJ (not shown) already agrees well with a sine function.

The angular dependence of the observable TST, *i.e.* the energy integral in Eq. (3), is plotted in Figs. 3(c) and (d). We observe strong deviations from a sine function at all temperatures considered. The skewness can be traced to multiple-reflection hot-spots caused by the interfacial resonances mentioned above. At room temperature the in-plane torkance peaks around 165° and the functional form can be fitted to an asymmetry parameter [28] of $\Lambda = 3.5$. This value is much larger than observed for the voltage-induced torque in metallic spin valves [29],

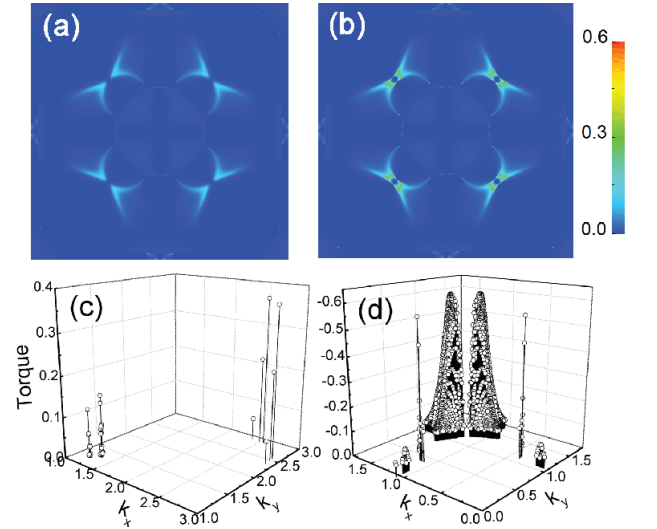


FIG. 4: k_{\parallel} -resolved electron transmission probability of (a) majority- and (b) minority-spin, and in-plane torkance from (c) majority- and (d) minority-spin channels in 3L MTJs with magnetization angle of 177.5° at energy $E_F - 0.0725$ eV. Majority (minority) are defined for the left lead. The integrated transmission probabilities are $4.6(6.3) \times 10^{-3} e^2/h$ and integrated in-plane torkances are 5.5×10^{-5} (-4.2×10^{-3}) eV for majority (minority) spins, respectively.

which should be beneficial for high-frequency generation [29]. We therefore suggest the possibility of efficient spin oscillators driven by heat flows through MTJs. The out-of-plane term is an effective field that dominates the in-plane term for angles $> 165^\circ$.

Fig. 3(e) and (f) displays the angular dependence of the spin transfer efficiency monitored by the ratio of the torque to charge current density for a given temperature bias $\Delta T = 1$ K. We find that the ratio (for both in-plane and out-of-plane terms) increases strongly close to the APC, for which the charge current is suppressed by the high spin polarization of the Fe-MgO interface [30].

The high spin transfer efficiency near the APC can be explained by multiple reflection due to resonant tunneling. In Fig. 4 resonant tunneling is observed in the APC at a chosen energy in both spin channels with a conductance polarization of 16%. Their contributions to the torkance are much larger, since the minority spin channel transfers 99% of the torkance due to its high interfacial electronic density of states. Here majority and minority spins are defined for the left lead. The resonance persists in the exact APC (Fig. 2(a)) but spin transfer vanishes for collinear magnetizations.

In Table I we compare TSTs equivalent to $\Delta T = 1$ K at $T_0 = 300$ K with electric STs for MTJs with 3, 5, and 7 MgO layers. The equivalent bias and current density of the thinnest barrier sample is much larger than that of the thicker one, which reflects the exponential decay of the conductance as a function of barrier thickness. ΔV_{eq}

TABLE I: Thermal torque T_{1K} per unit cell in nL MgO MTJs at $T = 300$ K and $\Delta T = 1$ K under closed and open (in brackets) circuit conditions for $\theta = 90^\circ$. $\Delta V_{eq} = T_{1K}/\tau_V$ is the equivalent bias. $\Delta V_{1K}/I_{1K}$ is the thermovoltage/thermoelectric current, T_V and I_V are electrically induced torque and current, respectively.

n	τ_V (mJ/V/m ²)	T_{1K}^* (nJm ⁻²)	ΔV_{eq} (mV)	ΔV_{1K} (mV)	T_{1K}/I_{1K} ($\hbar/2e$)	T_V/I_V ($\hbar/2e$)
3	0.72	-195(-232)	-0.27	0.052	-0.94	0.21
5	0.082	-3.32(-5.33)	-0.040	0.025	-0.84	0.46
7	0.011	-0.24(-0.062)	-0.021	-0.0154	3.58	0.98

*1 J V⁻¹ m⁻² = $3 \times 10^{18} (\hbar/2) \text{ k } \Omega^{-1} \text{ m}^{-2}$

is the ratio of thermal to electric torkance, which is larger for 3-MgO (1 K \sim 0.27 meV). ΔV_{1K} demonstrates that TSTs decrease faster than the electric STs when the barrier gets thicker. The sign change in ΔV_{1K} as a function of barrier thickness is attributed to that of the Seebeck coefficient. Moreover, the torque to current density ratio T/I is larger for the thermal than the electric case, indicating the superior efficiency of spin angular momentum transfer by temperature differences.

The TST is potentially useful for manipulating the magnetic configurations in MTJs with thin barriers. We estimate the critical temperature bias ΔT_c by comparing the TST with the measured torques at the critical voltage biases in CoFeB MTJ's at room temperature [31]. For 3ML MgO the switch from APC to PC should occur close to $\Delta T_c^{AP \rightarrow P} = 6.5$ K since then $|\mathbf{T}_{\Delta T}/\sin \theta| = 20 \times 10^{-6} \text{ J m}^{-2}$ equals the critical torque for electric switching. At $\Delta T_c^{P \rightarrow AP} = 56.5$ K, $|\mathbf{T}_{\Delta T}/\sin \theta| = 8.2 \times 10^{-6} \text{ J m}^{-2}$ equals the critical torque for electric PC to APC switching [31]. We note that τ_T is function of the global temperature that saturates around 275 K. Room temperature conditions are therefore favorable for thermal magnetization switching.

In an open circuit, the thermoelectric current vanishes, but not the thermospin current, thereby allowing transfer of angular momentum without transfer of charge. The thermal torque is even found to be larger in the closed compared to the open circuit, since the equivalent bias ΔV_{eq} and the thermovoltage ΔV_{1K} have opposite signs.

The spectral features due to resonances are sensitive to disorder. In Fig. 5 we show the angular-dependent torkance in 3-MgO with 10% OV's at both interfaces. We make comparison for two situations: one is at E_F , and another is at resonant peaks near to E_F . The resonant peaks in the clean samples at $E_F - 0.0725$ eV shift to lower energy (around $E_F - 0.055$ eV) in the presence of 10% OV as shown in Fig. 2, so different energies are chosen to compare clean and dirty situations. We observe that the disorder to a large extent restores the $\sin \theta$ angular dependence. The order of magnitude of the in-plane torkance of the ideal junctions at E_F is unmodified. The situation at the resonant peak is more complicated by a

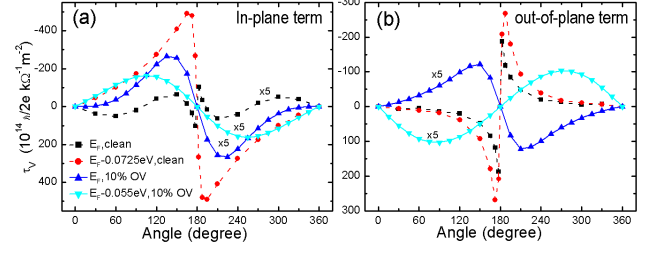


FIG. 5: Angular dependent (a) in-plane and (b) out-of-plane torkance in Fe-MgO(3L)-Fe(001) MTJs with specular and disordered interfaces at two selected energies, i.e., at the Fermi energy and at the resonance. Squares and circles are results for specular interfaces at E_F and $E_F - 0.0725$ eV, respectively; the up-pointing triangles and down-pointing triangles are disordered samples at E_F and $E_F - 0.055$ eV, respectively.

shift from $E_F - 0.0725$ eV (specular) to $E_F - 0.055$ eV (disordered) with decreased amplitude. A full calculation of the TST in the presence of OV disorder at room temperature is beyond our present computational capacity, but the two noted changes of the resonance will at least partly cancel each other.

In summary, we calculate TSTs of the order of 10^{-6} J m^{-2} in ultrathin Fe-MgO-Fe tunnel junctions at room temperature for a temperature bias of 10 K. A strong asymmetric angular dependence of TSTs is predicted for ballistic junctions. Based on these results we predict heat-flow-induced magnetization reversal and high frequency generation in magnetic tunnel junctions.

We gratefully acknowledge financial support from National Basic Research Program of China (973 Program) under the grant No. 2011CB921803, NSF-China grant No. 60825404, the Dutch FOM Foundation and EU-ICT-7 contract no. 257159 MACALO.

-
- [1] M. Johnson and R. H. Silsbee, Phys. Rev. B **35**, 4959 (1987); J. Shi *et al.*, Phys. Rev. B **54**, 15273(1996).
 - [2] G. E. W. Bauer, A. H. MacDonald, and S. Maekawa, Solid State Commun. **150**, 459 (2010).
 - [3] K. Uchida *et al.*, Nature **455**, 778 (2008); K. Uchida *et al.*, Nature **455**, 778 (2008); C. M. Jaworski *et al.*, Nature Mater. **9**, 898 (2010).
 - [4] A. Slachter *et al.*, Nature Phys. **6**, 879 (2010)
 - [5] A. Sugihara *et al.*, Appl. Phys. Exp. **3**, 065204 (2010); Nguyen Dang Vu, K. Sato, and H. Katayama-Yoshida, Appl. Phys. Express **4**, 015203 (2011).
 - [6] M. Hatami *et al.*, Phys. Rev. Lett. **99**, 066603 (2007), Phys. Rev. B **79**, 174426 (2009).
 - [7] H. Yu *et al.*, Phys. Rev. Lett. **104**, 146601 (2010)
 - [8] J. C. Slonczewski, Phys. Rev. B **82**, 054403 (2010).
 - [9] S. Yuasa *et al.*, Nature Mat. **3**, 868 (2004).
 - [10] S. S. P. Parkin *et al.*, Nat. Mat. **3**, 862 (2004).
 - [11] A. M. Deac *et al.*, Nat. Phys. **4**, 803 (2008).
 - [12] S. C. Oh *et al.*, Nat. Phys. **5**, 898 (2009).

- [13] R. Matsumoto *et al.*, Phys. Rev. B **80**, 174405 (2009).
- [14] M. H. Jung *et al.*, Phys. Rev. B **81**, 134419 (2010).
- [15] H. Yoda *et al.*, Current Appl. Phys. **10**, e87 (2010).
- [16] S. Ikeda *et al.*, Nature Mat. **9**, 721 (2010).
- [17] M. Czerner, M. Bachmann, and C. Heiliger, Phys. Rev. B **83**, 132405 (2011).
- [18] N. Liebing *et al.*, Phys. Rev. Lett. **107**, 177201 (2011);
M. Walter *et al.*, Nature Mater. **10**, 742 (2011).
- [19] J.-Ch. Le Breton, S. Sharma, H. Saito, S. Yuasa, R. Jansen. Nature **475**, 82 (2011).
- [20] J. A. Strosio *et al.*, Phys. Rev. Lett. **75**, 2960 (1995); O. Wunnicke *et al.*, Phys. Rev. B **65**, 064425(2002).
- [21] P. N. Butcher, J. Phys.: Condens. Matter **2**, 4869 (1990).
- [22] S. Wang, Y. Xu, and K. Xia, Phys. Rev. B **77**, 184430 (2008). Z. Yuan, S. Wang and K. Xia, Solid State Commun. **150**, 548 (2010).
- [23] Y. Ke, K. Xia, and H. Guo, Phys. Rev. Lett. **105**, 236801 (2010).
- [24] G. X. Miao *et al.*, Phys. Rev. Lett. **100**, 246803 (2008). P. G. Mather, J. C. Read, and R. A. Buhrman, Phys. Rev. B **73**, 205412 (2006).
- [25] J. Mathon, and A. Umerski, Phys. Rev. B **63**, 220403 (2001).
- [26] D. Wortmann, G. Bihlmayer, and S. Blügel, J. Phys.: Condens. Matter **16**, s5819 (2004).
- [27] I. Theodonis *et al.*, Phys. Rev. Lett. **97**, 237205 (2006).
- [28] J. C. Slonczewski, J. Magnet. Magnet. Mater. **247**, 324 (2002).
- [29] W.H. Rippard *et al.*, Phys. Rev. B **81**, 014426 (2010).
- [30] J.C. Slonczewski, J. Magnet. Magnet. Mater. **159**, L1 (1996); C. Heiliger and M. D. Stiles, Phys. Rev. Lett. **100**, 186805 (2008).
- [31] C. Wang *et al.*, Nat. Physics **7**, 496 (2011). We estimate the critical in-plane torque for magnetization reversal to be $|\mathbf{T}_{\Delta T}/\sin\theta| = 20 \times 10^{-6} \text{ J m}^{-2}$ for the AP-to-P transition at $-0.48(-0.2) \text{ V}$, corresponding to $\Delta T_c^{\text{AP} \rightarrow \text{P}}$ of 6.5 K at 300 K in our calculations; and $8.2 \times 10^{-6} \text{ J m}^{-2}$ for the P-to-AP transition at $0.48(0.2) \text{ V}$, corresponding to $\Delta T_c^{\text{P} \rightarrow \text{AP}}$ of 56.5 K at 300 K.